

## Hybrid Organic–Inorganic, Rod-Shaped Nanoresistors and Diodes

Sungho Park, Sung-Wook Chung, and Chad A. Mirkin\*

Department of Chemistry and Institute for Nanotechnology, Northwestern University, 2145 Sheridan Road, Evanston, Illinois 60208-3113

Received July 1, 2004; E-mail: camirkin@chem.northwestern.edu

Several routes have been developed for synthesizing quasi-one-dimensional (1D) nanostructures, many of which have interesting electronic, optical, and chemical sensor properties that derive from size, composition, and shape.<sup>1–7</sup> One-component systems are now quite common, but there are relatively few examples of methods for synthesizing multicomponent 1D materials made from both organic and inorganic materials.<sup>8–13</sup> Porous templates offer one the ability to routinely generate such structures through two distinct methods. Both rely on the use of electrochemistry to generate an initial block of metal from a plating solution. However, one utilizes layer-by-layer chemisorption processes<sup>10</sup> to build organic blocks on top of the preformed metal block while the other utilizes conducting polymer monomers combined with an appropriately applied potential to polymerize the monomer within the template at the metal block–solution interface.<sup>12</sup> An advantage of the latter approach is that it provides excellent control over the block length of the metal and organic regions of the structure, simply by controlling the number of coulombs that are passed in the experiment. Herein, we present an approach, based upon this synthetic strategy, for preparing hybrid multicomponent (i.e. organic–inorganic) nanorods that have either diode or resistor properties that derive from their compositions and spatial distribution of the different compositional blocks.

In a typical experiment, segmented metal–polymer nanorods ( $d = 324 \text{ nm} (\pm 32)$ ) were synthesized by electrochemical deposition of gold into alumina templates, followed by electrochemical polymerization of pyrrole (Ppy) (Supporting Information (SI)). The length of each block can be controlled by monitoring the charge passed during the electrodeposition process.<sup>12</sup> Other metals (e.g. Ag and Cd) with low work functions and inorganic semiconductors (e.g. CdSe), also can be deposited on top of the polymer block and polyaniline can be used in place of polypyrrole (see SI, Scheme 1). This allows one to prepare multicomponent rod structures with tailorable electronic properties that derive from the choice of the individual compositional blocks.

For the Au–Ppy–Au system, one can see dark Ppy domains sandwiched between two bright segments of gold (Figure 1A). Single nanorod devices were prepared for electrical characterization at different temperatures by depositing multicomponent Au–Ppy–Au nanorods on top of a microelectrode array, Figure 2A (inset). Multiple individually addressable microelectrodes allow one to electronically address the nanostructure at different points along its long axis. The Au portions of the nanostructure (contacts 1–2 and 3–4) exhibit linear  $I$ – $V$  characteristics and bulk metallic behavior at room temperature. Linear  $I$ – $V$  plots over a voltage range from  $-1$  to  $+1$  V demonstrate Ohmic behavior. Significantly,  $I$ – $V$  measurements across the Ppy block of the Au–Ppy–Au nanorod (2–3 and 1–4 contacts, Figure 2A) also exhibit a highly reproducible, linear response at room temperature but nonlinear behavior at low temperature ( $< 175 \text{ K}$ ), characteristic of a semiconductor, Figure 2B.

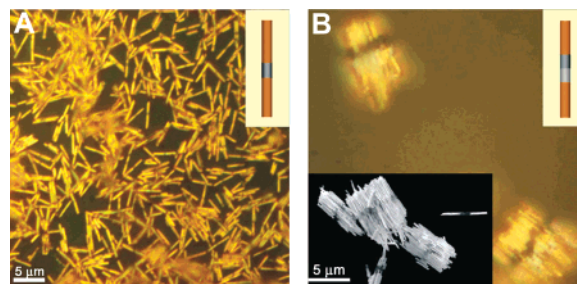


**Figure 1.** (A) Optical microscope image of Au–Ppy–Au rods. (B) Optical microscope image of Au–Ppy–Cd–Au rods. The lower left inset shows the corresponding field emission scanning electron microscopy (FESEM) image.

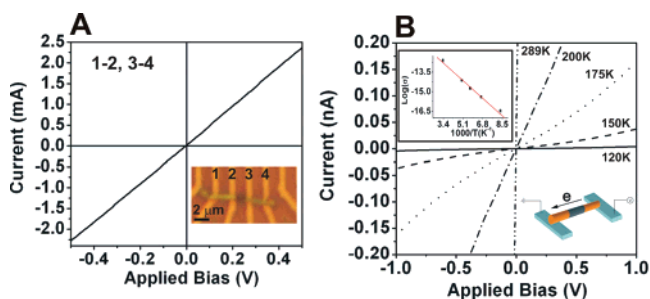


**Figure 2.** (A) Current–voltage ( $I$ – $V$ ) measurement for the gold blocks (1–2, 3–4) within a single nanorod at room temperature. Inset shows the optical microscope image (mag. 1000 $\times$ ) of a single Au–Ppy–Au rod on prefabricated microelectrodes. (B) Temperature-dependent  $I$ – $V$  curves for measurements across electrodes 2 and 3. The upper left inset is a plot of  $\log \sigma(T)$  vs  $1/T$ , showing a linear response ( $\sigma = \sigma_0 \exp(-E_a/kT)$ ,  $\sigma$ : conductivity,  $T$ : temperature). The slope is proportional to the activation energy ( $E_a$ ) which is  $\sim 0.07 \text{ eV}$ .

Analysis of the  $I$ – $V$  curves and the corresponding electrical conductivities provides two important observations. First, the room-temperature conductivity of the polymer block ( $\sim 3 \text{ mS}\cdot\text{cm}^{-1}$ ), is 6 orders of magnitude lower than the metallic blocks, and all data are consistent with Ohmic contact<sup>14,15</sup> between the Ppy–Au junctions. Indeed, the inner polymer blocks dictate the electrical properties of the hybrid three-component system, and the two Au blocks function simply as electrical leads to the microscopic circuitry. Second, the  $I$ – $V$  response for the Au–Ppy–Au nanorod becomes slightly nonlinear as the temperature decreases (Figure 2B). Such nanorods exhibit an Arrhenius-type temperature dependence with respect to conductivity, characteristic of thermally activated charge transport within the block of Ppy (Figure 2B inset). The semiconducting behavior of the Au–Ppy–Au nanorods is reminiscent of what has been observed for electrochemically polymerized bulk Ppy films. The experimentally determined activation energy ( $E_a = \sim 0.07 \text{ eV}$ ) of the Au–Ppy–Au nanorod is in good agreement with the values reported for a moderately doped bulk Ppy film and a nanotubular thin film structure (Figure 2B inset).<sup>16,17</sup> Since the polymer blocks for the nanostructures

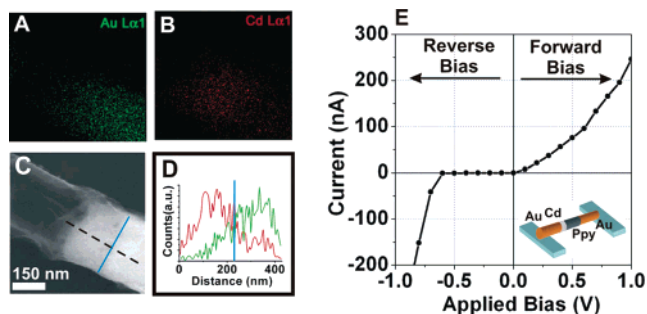


**Figure 3.** Images of EDS mapping for (A) Au and (B) Cd domains in a single Au–Ppy–Cd–Au rod. (C) FESEM image of the rod. (D) Graph of the X-ray profile for Cd and Au domains over the dashed trace shown in the image represented in C. The red line represents Cd X-ray counts, and the green line is a measurement of Au counts. The blue line in image (C) shows the junction formed between the Cd and Au domains. (E)  $I$ – $V$  characteristics for a single Au–Ppy–Cd–Au rod at room temperature.

discussed herein were generated by oxidative polymerization, they are p-type (vide infra).

Four-segment nanorods (Au–Ppy–Cd–Au) also can be prepared via an analogous procedure (see SI). The optical microscopy and FESEM images of such rods exhibit clear contrast between the three different chemical compositions (bright gold ends, dark Ppy, and white Cd), Figure 1B. The chemical composition of each inorganic block has been confirmed by energy-dispersive X-ray spectroscopy (EDS) elemental mapping experiments, Figure 3A–D. The FESEM of an individual rod clearly shows two interfaces (from left to right), between the Ppy and Cd blocks and between the Cd and Au blocks, Figure 3C. The EDS analysis of the dotted region in Figure 3C exhibits the characteristic elemental signatures for Cd and Au, Figure 3D. All data are consistent with the asymmetric junction structure within the single nanorod.

$I$ – $V$  measurements on devices constructed from single Au–Ppy–Cd–Au rods exhibit “diode” behavior at room temperature, Figure 3E. The typical response is asymmetric and non-Ohmic. In the forward bias, there is a positive voltage on the Au block adjacent to the Ppy and negative potential on the Au block interfaced with the Cd block. Therefore, holes move from the Ppy block to the Cd block during the forward bias. In reverse bias, current does not flow until the bias overcomes the breakdown potential ( $-0.61$  V). The turn-on voltage for these diode nanorods is approximately 0.15 V, almost  $\sim 1$  V lower than rods prepared thus far via the layer-by-layer assembly method.<sup>10</sup> The rectifying ratio (i.e., forward bias current/reverse bias current) is  $\sim 200$  at  $\pm 0.6$  V. The  $I$ – $V$  characteristics of the Au–Ppy–Cd–Au nanorods at room temperature suggest that a Schottky-like junction is formed at Ppy/Cd due to the difference in work functions of the two materials and an Ohmic junction at the Ppy/Au interface due to the similarity in work functions for the two materials.<sup>14,16,18,19</sup> By fitting the experimental  $I$ – $V$  responses to the model for metal semiconductor Schottky junctions,<sup>14,18</sup> a barrier height ( $\Phi_{\text{BH}}$ ) for the Ppy/Cd junction was determined to be  $\sim 0.68$  eV and is in good agreement with the reported values of electrochemically polymerized bulk Ppy/In junctions.<sup>16</sup>

This manuscript demonstrates that one can systematically synthesize multicomponent rodlike structures that contain metals, inorganic semiconductors, and conducting polymers via template-assisted in situ electrochemical deposition, and that such rod structures can be tailored through choice of block composition to exhibit resistor or diode like behavior in the context of an integrated microelectrode device. The approach can be contrasted with the alternative layer-by-layer approach for synthesizing multicomponent rod structures<sup>10</sup> in two ways. First, the electrochemical approach

offers greater control over the architectural parameters of the resulting structures (in particular block length). Second, the properties (e.g., turn-on voltages) of the resulting structures substantially differ, even when comparable materials are used. We believe the reason for this is that the junctions formed in the layer-by-layer approach are less well defined because the active materials are introduced as a polymer particle dispersion with little control over where the active interface is formed. The limitation of the electrochemical approach is that only conducting materials can be deposited within the pores. Regardless, this is a powerful method for deliberately producing structures with desirable electrical properties with a straightforward synthetic procedure that offers a high degree of reproducibility. These structures could be useful for a wide range of electronic and sensor devices, and efforts to explore such opportunities are underway.

**Acknowledgment.** C.A.M. acknowledges the NSF NSEC program, AFOSR, and DARPA for support of this research.

**Supporting Information Available:** Typical experimental procedures for making nanorods and electrical measurements. This material is available free of charge via the Internet at <http://pubs.acs.org>.

## References

- (1) Iijima, S.; Ichihashi, T. *Nature* **1993**, *363*, 603–605.
- (2) Thess, A.; Lee, R.; Nikolaev, P.; Dai, H. J.; Petit, P.; Robert, J.; Xu, C. H.; Lee, Y. H.; Kim, S. G.; Rinzler, A. G.; Colbert, D. T.; Scuseria, G. E.; Tomanek, D.; Fischer, J. E.; Smalley, R. E. *Science* **1996**, *273*, 483–487.
- (3) Heath, J. R.; Legoues, F. K. *Chem. Phys. Lett.* **1993**, *208*, 263–268.
- (4) Morales, A. M.; Lieber, C. M. *Science* **1998**, *279*, 208–211.
- (5) Martin, C. R. *Science* **1994**, *266*, 1961–1966.
- (6) Martin, C. R. *Acc. Chem. Res.* **1995**, *28*, 61–68.
- (7) Routkevitch, D.; Haslett, T. L.; Ryan, L.; Bigioni, T.; Douketis, C.; Moskovits, M. *Chem. Phys.* **1996**, *210*, 343–352.
- (8) Gudiksen, M. S.; Lathon, L. J.; Wang, J.; Smith, D. C.; Lieber, C. M. *Nature* **2002**, *415*, 617–620.
- (9) Lee, K.-B.; Park, S.; Mirkin, C. A. *Angew. Chem., Int. Ed.* **2004**, *43*, 3048.
- (10) Kovtyukhova, N. I.; Martin, B. R.; Mbindyo, J. K. N.; Smith, P. A.; Razavi, B.; Mayer, T. S.; Mallouk, T. E. *J. Phys. Chem. B* **2001**, *105*, 8762–8769.
- (11) Pena, D. J.; Mbindyo, J. K. N.; Carado, A. J.; Mallouk, T. E.; Keating, C. D.; Razavi, B.; Mayer, T. S. *J. Phys. Chem. B* **2002**, *106*, 7458–7462.
- (12) Park, S.; Lim, J. H.; Chung, S.-W.; Mirkin, C. A. *Science* **2004**, *303*, 348–351.
- (13) Nicewarner-Pena, S. R.; Freeman, R. G.; Reiss, B. D.; He, L.; Pena, D. J.; Walton, I. D.; Cromer, R.; Keating, C. D.; Natan, M. J. *Science* **2001**, *294*, 137–141.
- (14) Abthagir, P. S.; Saraswathi, R. *J. Appl. Polym. Sci.* **2001**, *81*, 2127–2135.
- (15)  $I$ – $V$  characteristics for the devices in Figure 2B show a slight nonlinearity at lower temperatures although they are highly linear at room temperature, as would be expected for a Schottky barrier. However, a Schottky barrier of a moderately doped p-type Ppy/Au junction would be expected to be quite small because the work functions of the two materials are quite similar. Therefore, the Au and semiconducting Ppy make an Ohmic-like contact. See ref 14 for a comparison of reported performance values for various bulk metal/Ppy junctions.
- (16) Watanabe, A.; Murakami, S.; Mori, K.; Kashiwaba, Y. *Macromolecules* **1989**, *22*, 4231–4235.
- (17) Park, J. G.; Kim, B.; Lee, S. H.; Park, Y. W. *Thin Solid Films* **2003**, *438*, 118–122.
- (18) Sze, S. M. *Physics of Semiconductor Devices*, 2nd ed.; Wiley: New York, 1981.
- (19) The difference in work function ( $\Delta\Phi$ ) between that for a metal such as Cd and that for a moderately doped p-type semiconducting Ppy is  $\sim 0.68$  eV, which is larger than that for Au and Ppy ( $\Delta\Phi(\text{Au–Ppy}) \approx 0.1$  eV) based on the assumption that the work function of an electrochemically polymerized Ppy film with a similar doping level is 4.9–5.1 eV, reported in refs 14 and 16.

JA046077V